A Method to Analyze How Various Parts of Clouds Influence Each Other's Brightness

Tamás Várnai and Alexander Marshak
Joint Center for Earth Systems Technology of
NASA Goddard Space Flight Center and
University of Maryland, Baltimore County

Prepared for the Journal of Geophysical Research—Atmospheres

August 31, 2001

Corresponding author address: Tamás Várnai, Code 913, NASA GSFC, Greenbelt, MD 20771, USA. E-mail: varnai@climate.gsfc.nasa.gov

Abstract

This paper proposes a method for obtaining new information on 3D radiative effects that arise from horizontal radiative interactions in heterogeneous clouds. Unlike current radiative transfer models, it can not only calculate how 3D effects change radiative quantities at any given point, but can also determine which areas contribute to these 3D effects, to what degree, and through what mechanisms. After describing the proposed method, the paper illustrates its new capabilities both for detailed case studies and for the statistical processing of large datasets. Because the proposed method makes it possible, for the first time, to link a particular change in cloud properties to the resulting 3D effect, in future studies it can be used to develop new radiative transfer parameterizations that would consider 3D effects in practical applications currently limited to 1D theory—such as remote sensing of cloud properties and dynamical cloud modeling.

1. Introduction

Current practical applications of calculating solar radiative transfer in clouds—such as cloud remote sensing and dynamical cloud models—rely on one-dimensional (*1D*) radiative transfer theory. This means that the calculations do not consider horizontal processes, that is, the three-dimensional (*3D*) radiative interactions between areas that have different cloud properties. Unfortunately, while the 1D assumption makes the calculations much more simple and fast, it can also cause significant errors in the case of heterogeneous clouds. For example, 1D cloud property retrievals based on satellite measurements can yield clouds that are too thin or too thick, too smooth or too structured, artificially anisotropic, or asymmetric (Marshak et al. 1995; Loeb and Davies 1996; Zuidema and Evans 1998; Várnai 2000). In addition, 1D calculations can have large errors in calculations of radiative fluxes and absorption values (e.g., Davies et al. 1984; Barker and Davies 1992; Marshak et al. 1999), thus resulting in inaccurate radiative heating rates in dynamical cloud models (e.g., O'Hirok and Gauthier 1998). Finally, 3D effects can also influence some chemical processes by changing the actinic fluxes that affect photodissociation rates (Los et al. 1997).

Ever since the first theoretical studies raised the issue of 3D radiative effects in the mid-1970s (Busygin 1973, McKee and Cox 1974), theoretical calculations have provided numerous important insights into these effects. The theoretical studies calculated the 3D effects indirectly, by comparing results when 3D effects were taken into account (3D calculations) and when they were not (1D calculations). Unfortunately, this indirect approach of detecting 3D effects from their imprint on the calculated

radiation fields puts some limitations on the information that can be obtained. For example, although the calculations can determine the overall influence of 3D effects on the brightness of a particular pixel, they cannot quantitatively address questions about their causes: Why is a certain pixel as bright as it is? What areas influence its brightness, to what degree, and through what mechanisms?

Currently, such questions cannot be answered even in a statistical sense, because 3D processes acting at one spatial scale can influence brightness variability at another scale. As a result, one cannot identify the scales at which 3D interactions occur by determining how 3D effects change brightness variability at each scale. This problem can be illustrated through a simple example, in which the only 3D effect is that cloud geometry changes the direct solar illumination at each point. This direct illumination depends on whether a pixel is on a slope tilted toward or away from the sun, which can be measured by the difference in geometrical—and assuming constant microphysics, optical—thickness between a pixel and its neighbor in front of it. In other words, the 3D effect in our example is proportional to the local gradient of cloud optical thickness. Fig. 1 shows that in this case, the small-scale interaction between neighboring pixels change the phase and amplitude of large-scale brightness variability.

In contrast to current, indirect methods, this paper presents a theoretical approach that can detect 3D effects directly as they modify the flow of radiation inside the cloud field. As a result, the proposed technique can not only calculate the combined effect a pixel's surroundings have on its brightness, but can also determine how specific areas contribute to the combined effect—to what degree, and through what mechanisms.

In examining the flow of radiation inside cloud fields the proposed technique is somewhat similar to the approach developed by Várnai and Davies (1999). However, while their approach examined radiative processes only in a scene-averaged sense, the technique proposed here can also give information on the spatial distribution of 3D radiative effects.

The new capabilities of the proposed method can not only provide us a more thorough understanding of 3D radiative processes, but in future studies it can also help in the interpretation of remote sensing measurements, and in developing parameterizations of 3D radiative fluxes and absorption values for dynamical cloud models.

The outline of this paper is as follows. First, Section 2 describes the proposed theoretical approach, then Section 3 illustrates the method's capabilities through several examples. Finally, Section 4 offers a brief summary and some concluding remarks.

2. Proposed technique

2.1 Basic definitions and requirements

While the proposed approach can be applied to examine any radiative quantity (i.e., radiances, fluxes and absorption values), this paper will describe the new technique using nadir reflectance (R) as an example. The reflectance is defined by the equation

$$R = \frac{\pi \cdot I}{\mu_0 \cdot F}, \tag{1}$$

where π is the geometric constant, I is the nadir radiance, μ_0 is the cosine of the solar zenith angle, and F is the solar irradiance. For the sake of simplicity, this reflectance will sometimes be referred to as "brightness".

The influence of 3D effects on the brightness of an area A (ΔR^A) is then defined as

$$\Delta R^A = R^A_{3D} - R^A_{1D}, \tag{2}$$

where R^A_{3D} and R^A_{1D} are the brightnesses calculated using 3D and 1D theory, respectively.

If we try to describe how various areas contribute to the total 3D effect changing the brightness of area A (that is, to ΔR^A), we need to define this contribution in a such way that its values satisfy two basic criteria.

Criterion I. *Once we calculate the contributions of any areas B and C, we need to know how these individual contributions can be combined.* This criterion is needed to ensure that the influence of large areas—or even of the entire cloud field—can be explained by considering the contributions of its various parts.

Criterion II. *The calculated contribution values should reflect how various areas affect the flow of radiation.* This criterion is needed to ensure that the results make sense physically.

Unfortunately, the two seemingly most straightforward approaches to determining various areas' influence on each other do not satisfy these criteria (see Appendix A), and so they cannot be used to determine how various areas contribute to the overall 3D effect. These two approaches are:

a) Examining how sensitive R^A is to changes in the properties of area B, and

b) Comparing the amount of scattering or absorption that occurs at B in the 1D and 3D cases.

While our goal is to attribute 3D effects to various areas, we should not forget that areas do not act in isolation: the influence of an area also depends on what other areas along the path of radiation do. For example, the properties of B may have a large influence on the brightness of A if the areas between A and B are transparent, but may have a negligible impact if the areas between A and B are so dense that they hardly allow any radiation through. Therefore the influence of B on A should be determined considering not only the properties of A and B, but also the entire path along which the radiation arrives from the sun, moves to B, and then goes to A. Accordingly, the technique proposed in this paper considers entire paths along which the radiation contributing to R^A can travel, and determines how 3D effects that occur at B influence the flow of radiation along each path. It performs the calculations in the following six steps:

1. Define a relevant set of paths along which radiation coming from the sun can reach A and contribute to R^A.

2. Calculate the overall influence of 3D effects along each path.

3. Select a representative subset of the paths that is suitable for calculating each area's influence.

4. Determine how areas along each path contribute to the overall 3D effect along that path.

5. Identify the mechanism of the 3D effects caused by each area along each path.

6. In order to obtain the areas' overall effects, combine the results obtained for each individual path.

These six steps are described in detail in Section 2.2.

2.2 Steps of the proposed technique

2.2.1 Step 1. Define a relevant set of paths along which radiation coming from the sun can reach A and contribute to R^A.

While there are several excellent 3D techniques that can calculate the spatial distribution of radiative quantities (e.g., Gabriel et al. 1993; Evans 1997), only the Monte Carlo approach can obtain the paths along which radiation travels. In principle, either forward or backward Monte Carlo simulations can be used to generate photon paths. In explaining the brightness of a particular pixel, however, backward simulations tend to be computationally more efficient, because in forward simulations one cannot tell in advance where the generated photon paths will lead, and so these simulations waste a lot of time simulating photon paths that do not even get close to our pixel. This waste cannot happen in backward calculations, which simulate a large number of photon paths "in reverse", tracing them backward from the pixel of our interest to the sun.

The photon paths used to obtain the numerical results of this paper were generated by the backward Monte Carlo model labeled "UMBC5" in the *Intercomparison of 3D Radiative Codes* (I3RC) project (see http://climate.gsfc.nasa.gov/I3RC).

Although 3D simulations can generate a representative set of paths along which radiation travels in the 3D scenes, this set alone is not sufficient to determine how 3D effects change the flow of radiation. Instead, two subsequent simulations need to be performed. First, a 3D simulation is used to generate the paths along which 3D effects enhance the flow of radiation, thereby increasing R^A. Then a 1D simulation is used to

generate the paths along which 3D effects reduce the flow of radiation, thereby reducing R^A. The 1D simulation is needed because the 3D simulation would undersample the paths along which 3D effects reduce the flow of radiation. For example, 3D simulations could not generate paths like the one in Fig. 2: since there is no scattering material at B in the 3D scene, the simulations could never put a scattering event at point B. As a result, 3D simulations would not notice that the hole at B reduces the radiation that would flow along this path; i.e., they would not notice that B causes a 3D effect that reduces R^A.

2.2.2. Step 2. *Calculate the overall influence of 3D effects along each path.*

Since all generated photon paths are used to examine how various areas influence the brightness of area A, let us make the notation slightly more simple by omitting the superscript A in the rest of Section 2.2. At the same time, let us introduce the sign $'$ to indicate when we are discussing not all the radiation moving toward A, but only the radiation following a single specific path. Using this notation, Equation (2) can be rewritten for individual paths as

$$\Delta R' = R'_{3D} - R'_{1D}. \tag{3}$$

For paths generated in the 3D simulation, R'_{3D} is calculated using standard Monte Carlo procedures. For these paths, R'_{1D} is calculated by comparing the probabilities that radiation can travel along the path in the 1D and 3D cases. To obtain these probabilities, we need to consider two factors:

i) The probability that the radiation arriving to a scattering point really gets scattered into the direction at which the path continues after the scattering. This

probability is determined by the product $\beta^s P$, where β^s is the volume scattering coefficient, and $P = P(\Theta)$ is the phase function value for the path's scattering angle (Θ).

ii) The probability that the radiation scattered at one point can reach the next scattering point along the specified path. This is determined by the optical thickness between the two subsequent scattering points.

Accordingly, R'_{1D} can be calculated from the equation

$$\frac{R'_{1D}}{R'_{3D}} = \prod_{i=1}^{N_s} \frac{\beta^s_{1D} P_{1D}}{\beta^s_{3D} P_{3D}}(r_i) \cdot \frac{\int_{sun}^{A} e^{-\beta_{1D} l} dl}{\int_{sun}^{A} e^{-\beta_{3D} l} dl}, \tag{4}$$

where N_s is the number of scattering events along the path, β is the volume extinction coefficient, and r_i is the position at the i^{th} scattering event along the path. Cloud properties with the subscript 3D indicate the properties of the 3D cloud field at point r_i, whereas the properties with the subscript 1D indicate the properties that would occur at point r_i if the entire cloud field had the same properties as pixel A (which is the assumption of 1D calculations). Finally, l indicates the position along the photon path, with the integration over l going along the entire path from the sun to A.

Once all the 3D paths are done, the same procedure is used for the paths defined in the 1D simulation—with the only difference that Eq. (4) is now used to get R'_{3D}.

2.2.3. Step 3. *Select a representative subset of defined paths that is suitable for calculating each area's influence.*

As mentioned at Step 1, the purpose of 3D Monte Carlo simulations is to generate paths along which 3D effects enhance the brightness of pixel A, while the purpose of 1D simulations is to generate paths along which 3D effects reduce R^A. However, the random procedures in the simulations unavoidably generate some paths with 3D effects opposite to the effects we are interested in: some 3D paths will have reductions and some 1D paths will have enhancements. Since these paths do not serve our purpose, we can simply discard them. (The suitability of each path is determined from the sign of $\Delta R'$ calculated in Step 2.) Then the remaining paths in the 3D and 1D simulations will indeed give truly representative samples of paths along which 3D effects enhance and reduce R^A, respectively.

2.2.4 Step 4. *Determine how areas along each path contribute to the overall 3D effect along that path.*

For each path, the influence of each area can be best characterized through the ratio (ρ') by which the areas enhance or reduce the flow of radiation along the path. The value of ρ' for an area B can be obtained by adapting Equation (4) to consider only regions inside B:

$$\rho'(B) = \prod_{i=1}^{N_s^B} \frac{\beta_{1D}^s P_{1D}}{\beta_{3D}^s P_{3D}}(r_i) \cdot \frac{\int_B e^{-\beta_{1D} l} dl}{\int_B e^{-\beta_{3D} l} dl}, \tag{5}$$

where N_s^B is the number of scattering events inside B, and the integration along the path l is also only inside B.

However, in its plain form ρ' is not a suitable measure for the area's influence. The problem is that if ρ' was used as is, one would not know how to combine the influences calculated for two arbitrary areas B and C after the results for all paths were summed up in Step 6. For example, the influences of B and C should be multiplied if they affected radiation that go through both of them, whereas the influences should be added up if B and C affected radiation approaching A through different paths (e.g., B affecting radiation coming from the left, and C affecting radiation coming from the right). This means that influence values calculated from plain ρ' values would contradict the first requirement mentioned in Section 2.1, that we need to know how we can combine the influences of various areas.

This problem can be avoided if we characterize the influence of an area through the logarithm of ρ'. For simplicity, this paper uses "natural" (e-based) logarithm, but the construction described below ensures that the results do not depend on our choice for the logarithm base (i.e., 10-based logarithms would give identical results). Using logarithms helps because the contributions of various areas always combine additively, since the ln ρ' values should be added even for areas that lie along the same photon paths:

$$\ln \rho'(B \cup C) = \ln\left[\rho'(B) \cdot \rho'(C)\right] = \ln \rho'(B) + \ln \rho'(C). \tag{6}$$

The contribution of B to the total 3D effect occurring along the path is then defined as

$$\Delta R'(B) = \Delta R' \frac{\ln \rho'(B)}{\sum_{N_p} \ln \rho'}, \tag{7}$$

where N_p is the number of pixels along the path.

This definition satisfies the two basic criteria mentioned in Section 2.1 the following way:

Criterion I. The influence of various areas can be combined by simple summation:

$$\Delta R'(B \cup C) = \Delta R'(B) + \Delta R'(C). \tag{8}$$

Criterion II. The definition reflects that 3D effects act by changing the flow of radiation by a factor that depends on the physical cloud properties.

The following examples illustrate that the technique attributes 3D effects to various areas in a reasonable way:

- If B has the same properties as A, the 3D effect attributed to it will be zero.
- If B reduces the radiation reaching A by a certain factor, and C reduces it further by the same factor, the overall reduction will be distributed evenly between the two areas.
- If areas B and C both reduce the radiation reaching A by 50%, their combined effect will be the same as the effect of a third area D that reduces it by another 75%.
- If B reduces the radiation reaching A by a certain factor, and C enhances it by the same factor, their combined effect will be zero.
- An area can have an enhancing effect even if the total 3D effect along the path reduces the flow of radiation. In this case the enhancement acts by mitigating the reduction caused by other areas along the path.
- If the total 3D effect along a path is exactly zero, the 3D effects occurring along the path are considered not influencing R^A, but changing the path of the radiation that would not get to A in any case (Fig. 3). Accordingly, the 3D influence is zero for all areas along the path.

*2.2.5. **Step 5.** Identify the mechanism of the 3D effects caused by each area along each path.*

The mechanisms of 3D effects can be identified by considering whether the 3D effects enhance or reduce the flow of radiation [i.e., $\Delta R'(B) < 0$ or $\Delta R'(B) > 0$], and whether they act by causing more extinction or less [e.g., $\beta_{3D} < \beta_{1D}$ or $\beta_{3D} > \beta_{1D}$]. In the case of conservative scattering (i.e., no absorption or emission), the combination of these two times two possibilities defines four basic mechanisms:

• **Enhancement by more scattering** (***EMS***). In this case the extra scattering acts to channel radiation to area *A* (Fig. 4a)—which is the channeling effect described in earlier studies (e.g., Cannon 1970; Davis and Marshak 2001).

• **Enhancement by less scattering** (***ELS***). In this case the reduced scattering allows more radiation to reach our pixel (Fig. 4b)—which is the process responsible for the side illumination effect described in earlier studies (e.g., Wendling 1977; Cahalan et al. 1994).

• **Reduction by more scattering** (***RMS***). In this case the extra scattering allows less radiation to reach *A* (Fig. 4c)—which is the shadowing effect described in earlier studies (e.g., Chambers et al., 1997; Zuidema and Evans 1998).

• **Reduction by less scattering** (***RLS***). In this case the reduced scattering allows some radiation to leak out of the paths leading to *A* (Fig. 4d)—which is the process responsible for the leakage effect described in earlier studies (e.g., Davies 1978; Kobayashi 1993).

When absorption or emission is also present, the additional mechanisms *Enhancement by less absorption* (ELA), *Reduction by more absorption* (RMA), *Enhancement by more emission* (EME), and *Reduction by less emission* (RLE) can be calculated in a straightforward way.

Let us note that although these mechanisms are somewhat related to the mechanisms defined by Várnai and Davies (1999), there are some important differences between the two sets of definitions. For example, Várnai and Davies (1999) defined a separate 1D case for each photon path (based on the cloud properties at the point where the photon entered the cloud field), whereas the new framework uses a single 1D reference case for all paths leading to our pixel. This difference makes the new approach more suitable for practical applications, for example in remote sensing.

The basic mechanisms described above influence individual pixels, and so they can be combined into two processes that change the structure of the brightness field. These two processes were described qualitatively in numerous earlier studies (e.g., Marshak et al. 1995; Davis et al. 1997; Oreopoulos et al. 2000)

• **Roughening**. The mechanisms ELS, RMS, ELA, and RMA act to increase the brightness difference between influencing and influenced pixels that we would expect from 1D theory, thereby roughening the brightness field. Mathematically:

$$Roughening = |ELS| + |RMS| + |ELA| + |RMA|. \quad (9)$$

• **Smoothing.** The mechanisms EMS, RLS, EME, and RLE act to reduce the brightness difference between influencing and influenced pixels that we would expect from 1D theory, thereby smoothing out the brightness field. Mathematically:

$$Smoothing = |EMS| + |RLS| + |EME| + |RLE|. \quad (10)$$

Finally, the sum of all eight pixel-level mechanisms gives the overall 3D effect:

$$\Delta R' = ELS + EMS + ELA + EME + RLS + RMS + RMA + RLE. \quad (11)$$

2.2.6 Step 6. *In order to obtain an area's overall effect, combine the results obtained for each individual path.*

This step can be described mathematically as

$$\Delta R(B) = \sum_{i=1}^{N_{\text{path}}} \Delta R_i'(B), \quad (12)$$

where N_{path} is the total number of all photon paths deemed suitable in Step 3, considering paths generated in both the 3D and 1D simulations.

In the end, the contribution values calculated from Eq. (12) can be interpreted through the following two sentences. *Summing up the influence of all areas gives the overall 3D effect,* ΔR^{A}. *If area B has a contribution X times larger than area C has, then a set of X number of areas having the same influence as C will have a combined effect equivalent to B's.* This second sentence is illustrated in Fig. 5, where areas B and C have equivalent contributions, and D has a contribution twice as large as either B or C.

3. Some results on the spatial distribution of 3D effects

This section describes some sample results that illustrate various ways in which the proposed method can give new insights into 3D radiative effects. The first few

examples are for the cloud field used in Case 4 of the I3RC project (see http://climate.gsfc.nasa.gov/I3RC). The cloud field (Fig. 6a) covers a $(3.84\ \mathrm{km})^2$ area at 30 m resolution. Following the specifications of Experiment 2 in the I3RC project, the calculations presented here assume no atmospheric effects, non-reflecting surface, Henyey-Greenstein scattering phase function, and 60° solar zenith angle with the sun on the left.

Figure 6b shows how various areas influence the brightness of an arbitrarily selected point A at row 57, column 90. Let us note that the values in the map are very small, because each number represents the contribution of an individual $(30\ \mathrm{m})^2$ pixel. Summed up over the entire scene, these values give the overall 3D effect of $\Delta R^{\mathrm{A}} = 0.128$ ($R^{\mathrm{A}}_{1\mathrm{D}} = 0.574$, $R^{\mathrm{A}}_{3\mathrm{D}} = 0.702$). The figure reveals that most of the 3D effects are caused by the thin areas right in front of A, and by the cloud bump right behind it. Still, even areas farther away have a discernible impact: in front, thin areas (B, C) enhance R^{A} through ELS, whereas sideways and behind, thick areas (D) increase R^{A} through EMS and thin areas (E, F) reduce it through RLS.

In addition to examining 3D effects that influence individual pixels, the proposed method can also give scene averaged results, by simply combining results obtained through moving the position of the influenced pixel across the scene. Table 1 displays the results of a such calculation regarding the magnitude of various 3D mechanisms. The results reveal that, perhaps somewhat surprisingly, the strongest mechanism in this scene is RLS, whereas the weakest one is RMS. Also, smoothing is somewhat stronger than roughening—which means that influencing pixels have a slight tendency to modify their surroundings' reflectance by nudging them closer to their own 1D reflectance.

We can learn further details on smoothing and roughening if we plot what net roughening (= roughening – smoothing) is caused by pixels at various distances from the influenced pixels. Fig. 7 shows that roughening works primarily in the solar plane (that is, pixels tend to feel roughening effects from pixels in front of them), whereas smoothing is much more isotropic. The difference suggests that roughening acts mainly by influencing the pixels' illumination by direct and low-order scattered sunlight, while smoothing is caused by diffusion due to multiple scattering. Also, the result is consistent with the results in Várnai (2001), which show that 3D effects make the reflectance field anisotropic, with stronger variability in the along-sun than in the cross-sun direction.

In addition to allowing detailed case studies of individual scenes, the proposed method can also provide statistical information for large sets of scenes. Fortunately, these calculations do not take longer than the calculations for individual scenes: in most cases we can build accurate statistics by combining quick, noisy results obtained for individual scenes. Such statistical results can be important in practical applications, particularly in the development of new radiative transfer parameterizations for either remote sensing or dynamical cloud models. Specifically, the statistical results can provide information on how the pixels' influence depends on various parameters, such as the properties of the influenced and influencing pixels and their position relative to each other. (The parameterizations could be further improved by also considering statistical parameters of the pixels' surroundings, especially along the most typical photon paths.)

To illustrate the kind of results the method can give, some sample calculations were performed to examine how pixels with $\tau = 10$ are influenced by pixels with $\tau = 5$ and $\tau = 15$ around them. For this, 5000 cloud fields were generated using the third fractal

cloud model described in Várnai and Marshak (2001) (the one based on the model of Evans (1993)). The goal was not to provide a climatologically representative statistics, only to cover a wide but realistic range of cloud properties. While all scenes cover (12.8 km)^2 areas at 100 m resolution, have a constant cloud base and a constant volume scattering coefficient of 30 km^{-1}, and use the I3RC C.1. scattering phase function, the other scene parameters were chosen randomly for each scene between the limits listed in Table 2. Next, 4 % of for all pixels with $9.75 < \tau < 10.25$ were selected from each of the scenes and 1000 1D and 1000 3D photon paths were simulated for each selected pixel. The results were then combined for all pixels and saved as a function of various parameters.

As a sample result, Fig. 8 shows the role of the pixels' position relative to each other. Panel a quantifies the intuitive trend that thin areas in front enhance a pixel's brightness while thin areas behind reduce it, while Panel b shows that the trends reverse for thick areas In addition, the figure also shows that the pixels' influence on each other drops much more quickly with their distance in the cross-sun direction than with their distance in the along-sun direction. This is because radiation arriving from the sun travels mainly in the along-sun direction before multiple scattering can direct some of it into cross-sun directions. Also, the comparison of Panels a and b reveals that τ changes of the same magnitude ($|\Delta\tau| = 5$) have stronger radiative effects if the pixel in front is thicker, rather than thinner. Finally, the figure reveals that the same τ-difference is more effective if it occurs over larger distances, i.e., in less steep slopes. On sunlit slopes this is because too steep slopes allow some incoming direct radiation to descend to such low altitudes that they need to travel some more horizontal distance before they can turn around and

emerge from the cloud top. On slopes facing away from the sun, too steep cloud bumps are less effective because they do not only shadow our pixel, but also steer some such radiation toward it that would have passed over the top of our pixel without the bump's interference.

4. Summary

This paper proposed a method for obtaining new information on 3D radiative effects arising from horizontal radiative interactions in heterogeneous clouds. The goal was to overcome a limitation of current radiative transfer models that can calculate only how 3D effects change radiative quantities at any given point (for example, the point's visible brightness), but cannot quantitatively address questions about their causes, such as: *Why is a certain point as bright as it is? What areas influence its brightness, to what degree, and through what mechanisms?* The proposed method can address such questions by detecting 3D effects directly, as they modify the flow of radiation inside the cloud field. As a result, it can not only calculate the combined effect a point's surroundings have on its brightness, but can also determine how specific areas contribute to the combined effect—to what degree, and through what mechanisms.

The proposed method starts with Monte Carlo simulations that create a representative set of paths along which radiation could possibly reach the point whose brightness we are to explain. It then examines how areas enhance and reduce the flow of radiation along each path. The method recognizes that areas do not act in isolation, but rather that an area's influence depends on what other areas along the path are like. For

example, an area can strongly affect another one if the areas between them are transparent, but it cannot make much of a difference if the areas in between are so dense that they hardly allow any radiation through. Accordingly, the proposed method determines the influence of an area by considering both the ratio by which the area enhances or reduces the flow of radiation along a particular path, and also the way all areas combined change the flow along that path.

The paper argued that one needs to satisfy two basic criteria in order to determine in a meaningful way how each area contributes to the overall 3D effect. First, in order to explain the influence of larger areas, one needs to know how to combine the contribution values calculated for smaller areas. Second, the calculated contribution values should reflect how various areas affect the flow of radiation physically. These two criteria were then used to define the contribution values such that they can be interpreted through the following two sentences: First, summing up the contribution of all areas gives the overall 3D effect. Second, if area *B* has a contribution *X* times larger than area *C*, then *X* number of areas having the same influence as *C* will have a combined effect equivalent to *B*'s. For example, if *B* enhances the flow of radiation along a path by a factor of 3 (compared to the flow in a 1D, homogeneous cloud), and areas *C* and *D* enhance it further by factors of 3 and 9, respectively, then *B* and *C* should have equal contributions, and *D*'s contribution should be twice as large.

Finally, the method determined the mechanism of 3D effects caused by each area. For this, it provided quantitative definitions for 3D processes that were described qualitatively in earlier studies, for effects both on individual points (e.g., side illumination or shadowing) and on the structure of entire scenes (i.e., smoothing and roughening).

After describing the proposed method, the paper illustrated its new capabilities through several examples. First, a cloud field used in the I3RC project was examined in detail: 3D effects influencing a particular point were mapped out, and their mechanisms were also calculated. These sample results provided some new insights, for example that shadowing (termed here as "reduction by more scattering") was the weakest 3D mechanism even for a solar zenith angle of 60°.

Finally, some statistical results were also obtained for large sets of scenes. The results illustrated how the influence of one point on another depends on the points' positions relative to each other. Perhaps it is in generating such statistical results that the proposed method may become most useful in future studies: Because the method can link a cause to its effect for the first time (i.e., link a particular change in cloud properties to the resulting 3D radiative effect), it can be used in developing new radiative transfer parameterizations. These parameterizations could incorporate 3D effects into practical applications that are currently limited to 1D theory, for example into the remote sensing of cloud properties or into dynamical cloud modeling.

Acknowledgments. We appreciate funding for this research from the NASA EOS Project Science Office (under Grant NAG5-6675), and support from project scientist David O'C. Starr. We are also grateful to Laura Atwood for proofreading the manuscript.

Appendix A. Problems with two seemingly straightforward approaches for determining how various areas influence each other.

One straightforward approach would characterize the influence of various areas on R^A through sensitivity experiments that would determine how R^A changed if one by one, the properties of each surrounding area were switched from the 1D to the 3D case. Unfortunately this approach would not satisfy the first criterion mentioned in Section 2.1, because the results would not reveal how the sensitivities to individual areas should be combined to explain the overall 3D effect. For example, if the sensitivity results show that R^A is reduced from 1.0 to 0.75 when the properties of either area B or C are switched from the 1D to the 3D case, one could not tell what would happen if both B and C were switched to 3D simultaneously: The combined effect could be a reduction to either 0.5625 ($= 0.75^2$) or to 0.5, depending on whether or not the two areas affect the same stream of radiation that goes through both of them on the way to A.

Another straightforward approach would characterize various areas' influence on R^A by comparing the extinction of radiation traveling toward A in the 1D and 3D cases. In other words, this approach would use the magnitude of 3D effects that occurs in each area. Unfortunately this approach would not satisfy the second criterion mentioned in Section 2.1: It would not reflect how various areas affect the flow of radiation, and so it would give unreasonable results in some cases. One such example could be if pixel B contained slightly more absorbing material than pixel A, but pixel C would cast a dark shadow on both of them. This shadowing could reduce the absorption that actually occurs in B below the level of B's absorption in the 1D case (which has no shadowing). As a

result, the approach would declare that since less absorption occurs in area B in the 3D than in the 1D case, the 3D effect attributed to B is to enhance the brightness of pixel A. This result is clearly not meaningful, since we added more absorbing material to B when we switched from 1D to 3D, and the extra absorbing material cannot enhance the brightness of pixel A.

References

Barker, H. W., and J. A. Davies, 1992: Solar radiative fluxes for stochastic, scale-invariant broken cloud fields. *J. Atmos. Sci.*, **49**, 1115-1126.

Busygin, V. P., N. A. Yevstratov, and Ye. M. Feygelson, 1973: Optical properties of cumulus clouds, and radiative fluxes for cumulus cloud cover. *Izv. Acad. Sci. USSR, Atmos. & Oceanic Phys.*, **9**, 648-653.

Cahalan, R. F., W. L. Ridgway, and W. J. Wiscombe, 1994: Independent pixel and Monte Carlo estimates of stratocumulus albedo. *J. Atmos. Sci.*, **51**, 3776-3790.

Cannon, J. C., 1970: Line transfer in two dimensions. *Astrophys. J.*, **161**, 255-264.

Chambers, L. H., B. A. Wielicki, and K. F. Evans, 1997: Independent pixel and two-dimensional estimates of Landsat-derived cloud field albedo. *J. Atmos. Sci.*, **54**, 1525-1532.

Davies, R., 1978: The effect of finite geometry on the three-dimensional transfer of solar irradiance in clouds. *J. Atmos. Sci.*, **35**, 1712-1725.

Davies, R., W. L. Ridgway, and K.-E. Kim, 1984: Spectral absorption of solar radiation in cloudy atmospheres: A 20 cm-1 model. *J. Atmos. Sci.*, *41*, 2126-2137.

Davis, A. B., A. Marshak, R. F. Cahalan, W. J. Wiscombe, 1997: The Landsat scale break in stratocumulus as a three-dimensional radiative transfer effect: Implications for cloud remote sensing. *J. Atmos. Sci.*, **54**, 241-260.

Davis., A. B., and A. Marshak, 2001: Multiple scattering in clouds: Insights from three-dimensional diffusion/P_1 theory. *Nuclear Sci. and Engineering*, **137**, 251-280.

Evans, K. F., 1993: The spherical harmonics discrete ordinate method for three-dimensional atmospheric radiative transfer. *J. Atmos. Sci.*, **55**, 429-446.

Gabriel, P. M., S.-C. Tsay, and G. L. Stephens, 1993: A Fourier-Ricatti approach to radiative transfer. Part I: Foundations. *J. Atmos. Sci.*, **50**, 3125-3147.

Kobayashi, T., 1993: Effects due to cloud geometry on biases in the cloud albedo derived from radiance measurements. *J. Climate*, **6**, 120-128.

Loeb, N. G., and R. Davies, 1996: Observational evidence of plane parallel model biases: Apparent dependence of cloud optical depth on solar zenith angle. *J. Geophys. Res.*, **101**, 1621–1634.

Los, A., M. van Weele, and P. G. Duynkerke, 1997: Actinic fluxes in broken cloud fields. *J. Geophys. Res.*, **102**, 4257-4266.

Marshak, A., A. Davis, W. Wiscombe, and R. Cahalan, 1995: Radiative smoothing in fractal clouds. *J. Geophys. Res.*, **100**, 26,247-26,261.

Marshak, A., W. Wiscombe, A. Davis, L. Oreopoulos, and R. F. Cahalan, 1999: On the removal of the effect of horizontal fluxes in two-aircraft measurements of cloud absorption. *Quart. J. Roy. Meteor. Soc.*, **125**, 2153-2170.

McKee, T. B., and S. K. Cox, 1974: Scattering of visible radiation by finite clouds. *J. Atmos. Sci.*, **31**, 1885-1892.

O'Hirok, W., and C. Gautier, 1998: A three-dimensional radiative transfer model to investigate the solar radiation within a cloudy atmosphere. Part I: Spatial effects. *J. Atmos. Sci.*, **55**, 2162–2179.

Oreopoulos, L. A. Marshak, R. F. Cahalan, and G. Wen, 2000: Cloud three-dimensional effects evidenced in Landsat spatial power spectra and autocorrelation functions. *J. Geophys. Res.*, **105**, i4,777-14,788.

Várnai, T., 2000: Influence of three-dimensional radiative effects on the spatial distribution of shortwave cloud reflection. *J. Atmos. Sci.*, **57**, 216–229.

Várnai, T., and R. Davies, 1999: Effects of cloud heterogeneities on shortwave radiation: Comparison of cloud-top variability and internal heterogeneity. *J. Atmos. Sci.*, **56**, 4206–4223.

Wendling, P., 1977: Albedo and reflected radiance of horizontally inhomogeneous clouds. *J. Atmos. Sci.*, **34**, 642-650.

Zuidema P. and K. F. Evans, 1998. On the validity of the Independent Pixel Approximation for the boundary layer clouds observed during ASTEX. *J. Geophys. Res.*, **103**, 6059–6074.

Tables

Table 1. Scene-averaged magnitude of various 3D mechanisms

Mechanism	Magnitude
EMS	0.182
RMS	-0.132
ELS	0.329
RLS	-0.345
Smoothing	0.527
Roughening	0.461
Overall 3D effect	0.034

Table 2. Limits for various statistical cloud parameters.

Stationarity parameter (H)	0.3 – 0.45
Probability of overcast scenes	0.2
Cloud fraction for broken cloud scenes	0.3 – 1.0
Scene averaged optical thickness	5 - 15
ν (= Mean / St. dev)	4 - 25 for overcast scenes 1 – 5 for broken cloud scenes

Figure captions

Figure 1. Schematic graph illustrating that 3D effects acting at small scales can influence large-scale reflectance variability. The magnitude of 3D effects (ΔR) is defined as $\Delta R = c\frac{\delta\tau}{\delta x}$ with c being a constant. The true, 3D reflectance (R_{3D}) is then obtained as $R_{3D} = R_{1D} + \Delta R$, with $R_{1D} = R_{1D}(\tau)$ being the reflectance calculated using 1D theory.

Figure 2. A path along which radiation can travel in a 1D cloud, but not in a 3D scene.

Figure 3. A sample path (solid line) along which such 3D effects occur that are not considered to change the reflectance at pixel *A*. In the 1D case (in which all pixels have the same density as pixel *A*) some radiation coming from the sun follows the path only into pixel *C*, where it leaves the cloud without any scattering, as indicated by the dotted arrow. In the 3D case the extra droplets at *C* prevent this radiation to leave, and make it follow the path further, into pixel *B*. The low density at *B*, however, allows this extra radiation to leave the cloud without additional scattering, as indicated by the dashed arrow. In the end, the radiation reaching pixel *A* is the same in the 1D and 3D cases—and so 3D effects are considered changing not the reflectance of *A*, but whether the radiation not reaching *A* will follow the dotted or dashed arrows.

Figure 4. Examples of four mechanisms of 3D effects influencing R^A. The solid arrows indicate the path of radiation in the 3D cloud field; the dotted arrows indicate the path the radiation would follow in the 1D case (in which the entire scene has the same properties as pixel *A*).

Figure 5. Examples for situations where areas *B* and *C* have equal contributions to the 3D effect influencing the brightness of *A*, while *D* has a contribution twice as large as either *B* or *C*. Each arrow represents a path along which a unit amount of radiation would travel in the 1D case.

Figure 6. (a) Optical thickness distribution of the I3RC Case 4 cloud field. (b) Contribution of various areas to the overall 3D effect influencing the brightness of point *A*.

Figure 7. Scene averaged map of net roughening (= roughening – smoothing) as a function of the influencing pixels' position relative to the influenced pixel. Negative and positive along-sun distances indicate that the net roughening is caused by pixels in front or behind the influenced pixel, respectively.

Figure 8. Average influence of pixels with $\tau = 5$ (Panel a) and $\tau = 15$ (Panel b) on pixels with $\tau = 10$. Negative distances indicate that the influencing pixel is in front of the influenced one. The three lines show results for three different cross sun distance (csd) values between the influenced and influencing pixels.

Figures

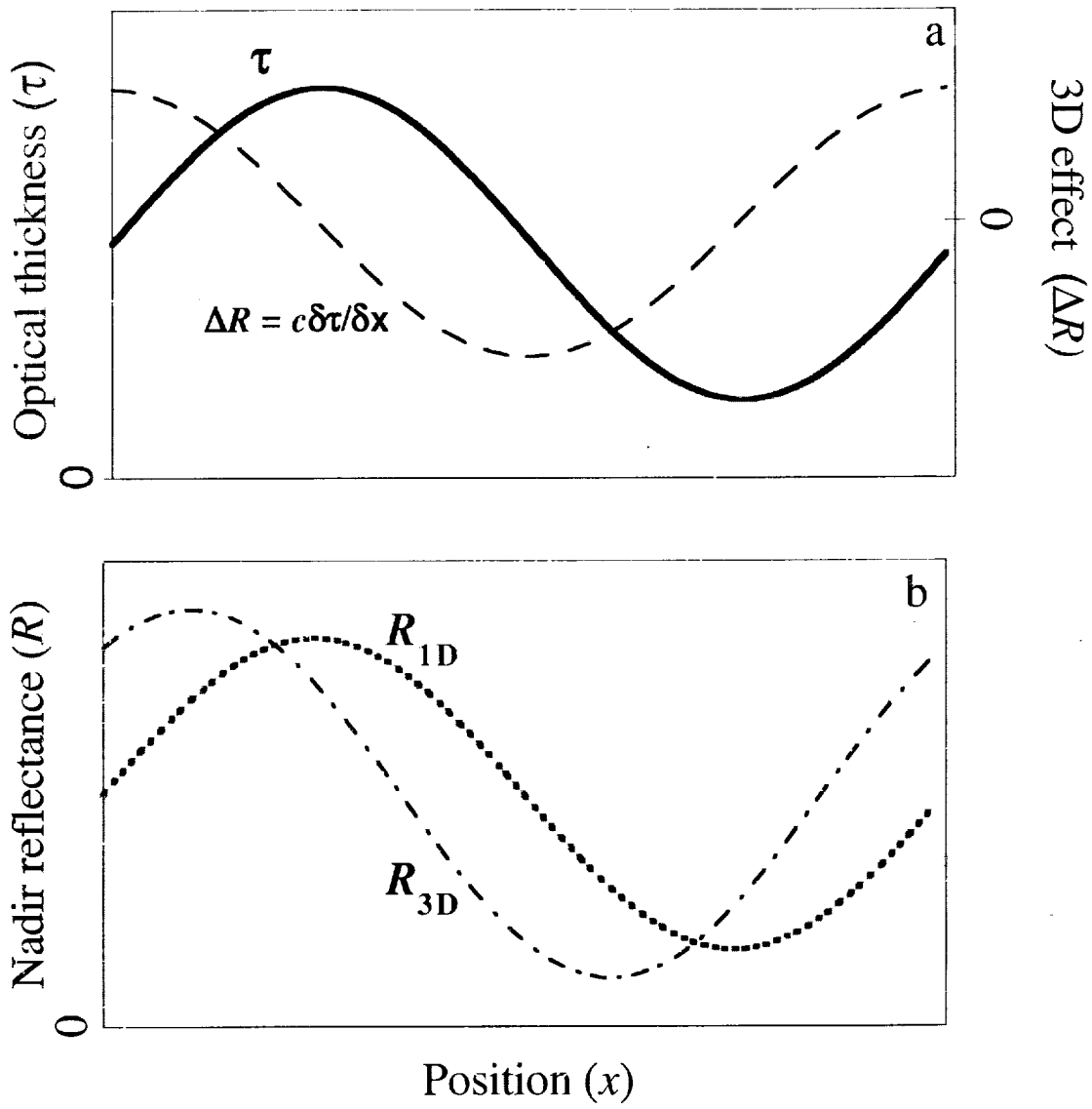

Figure 1.

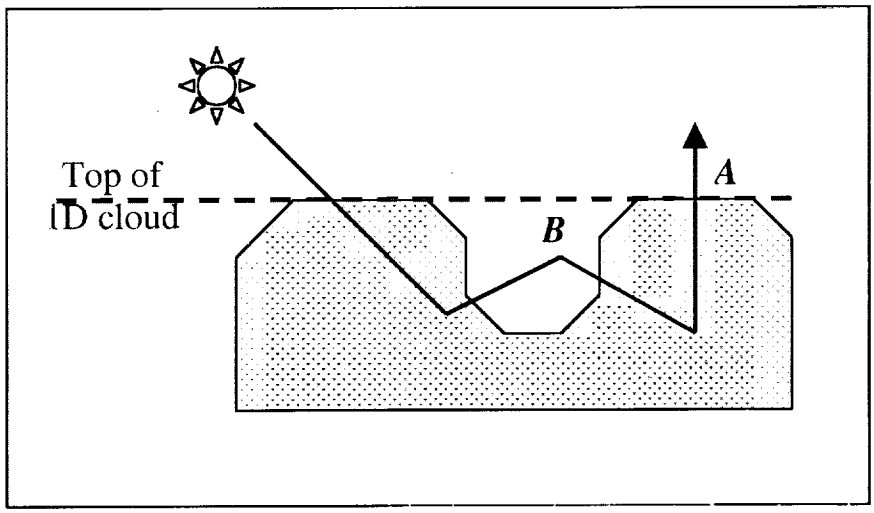

Figure 2.

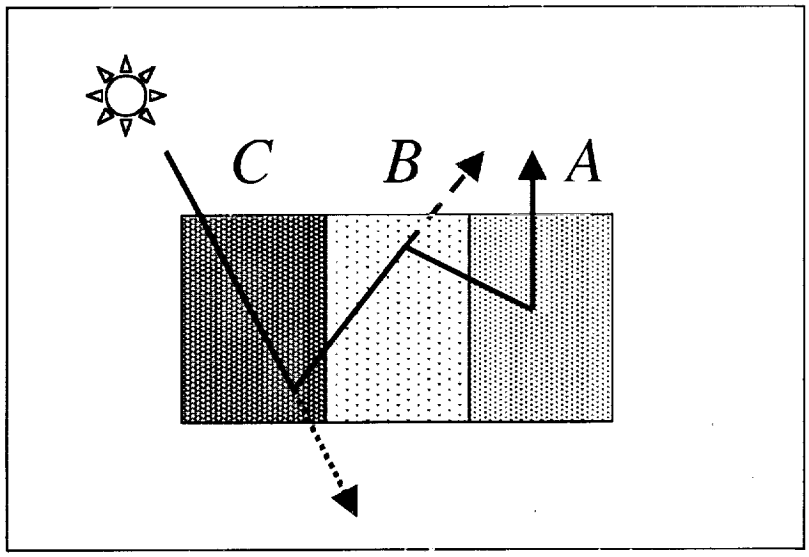

Figure 3.

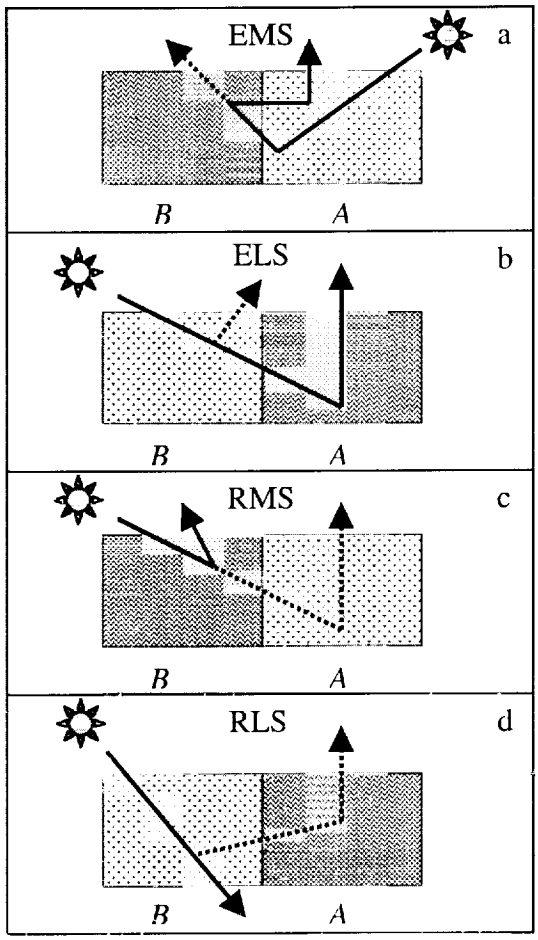

Figure 4.

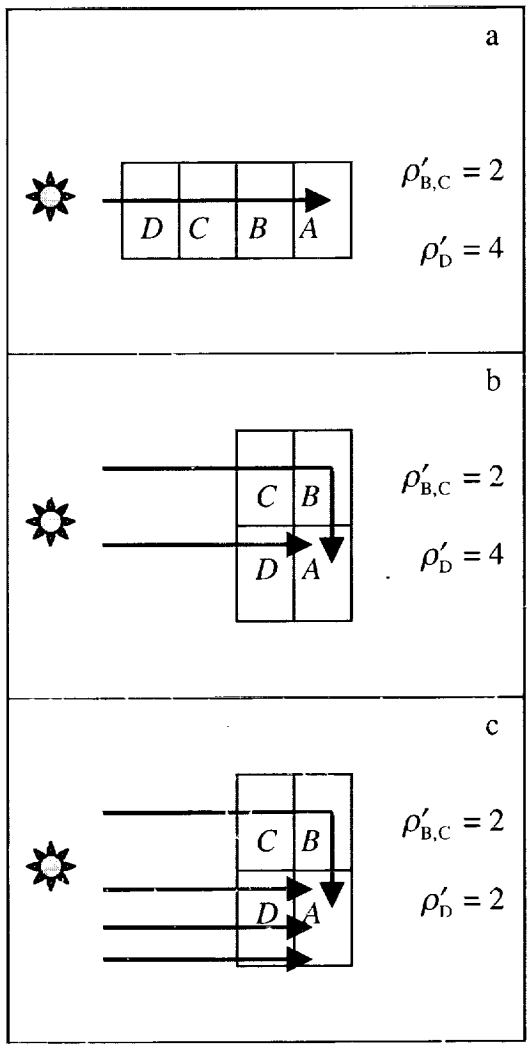

Figure 5.

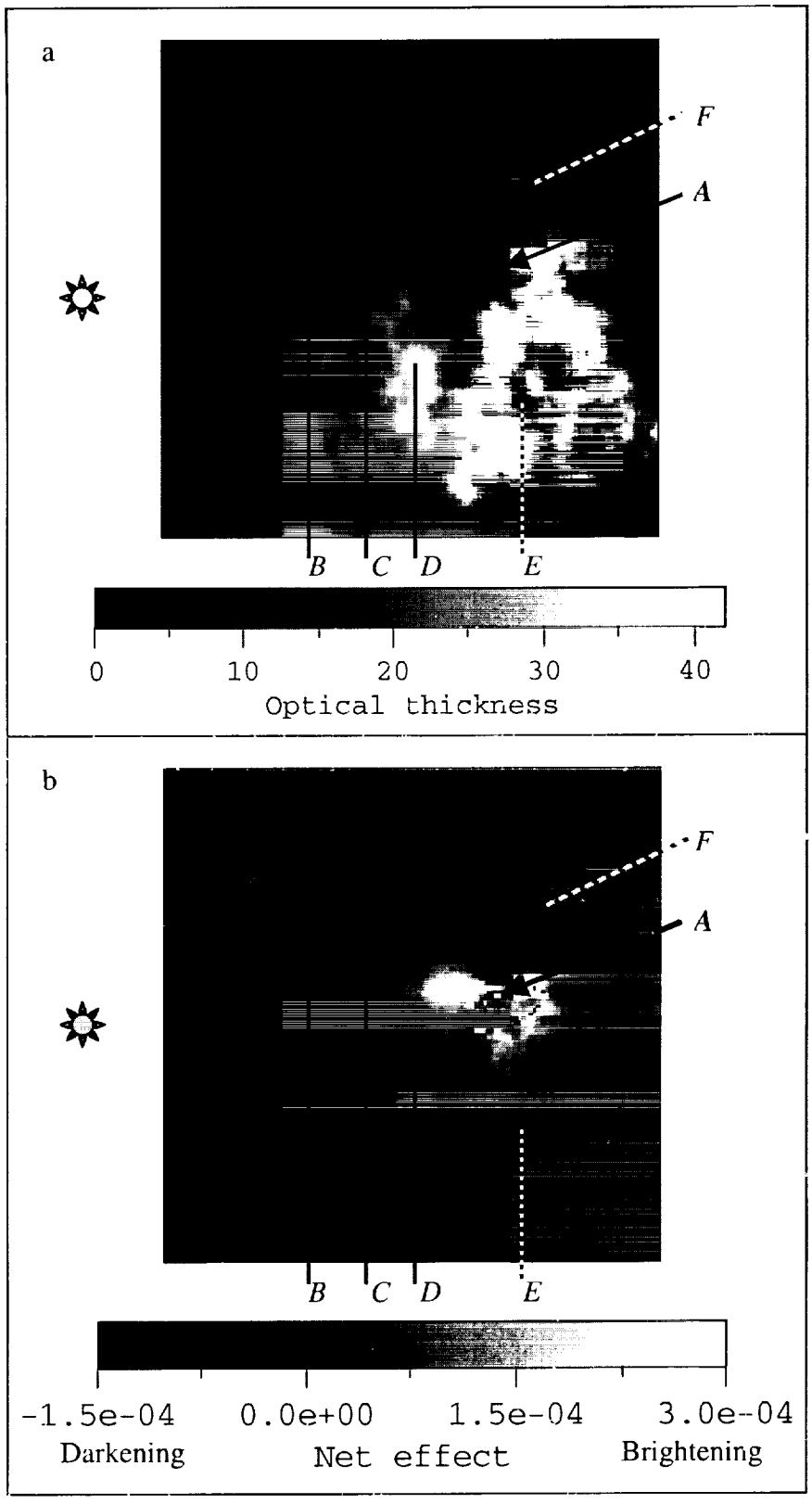
a
F
A
B
C
D
E
0
10
20
30
40
Optical thickness
b
F
A
B
C
D
E
-1.5e-04
0.0e+00
1.5e-04
3.0e-04
Darkening
Net effect
Brightening

Figure 6.

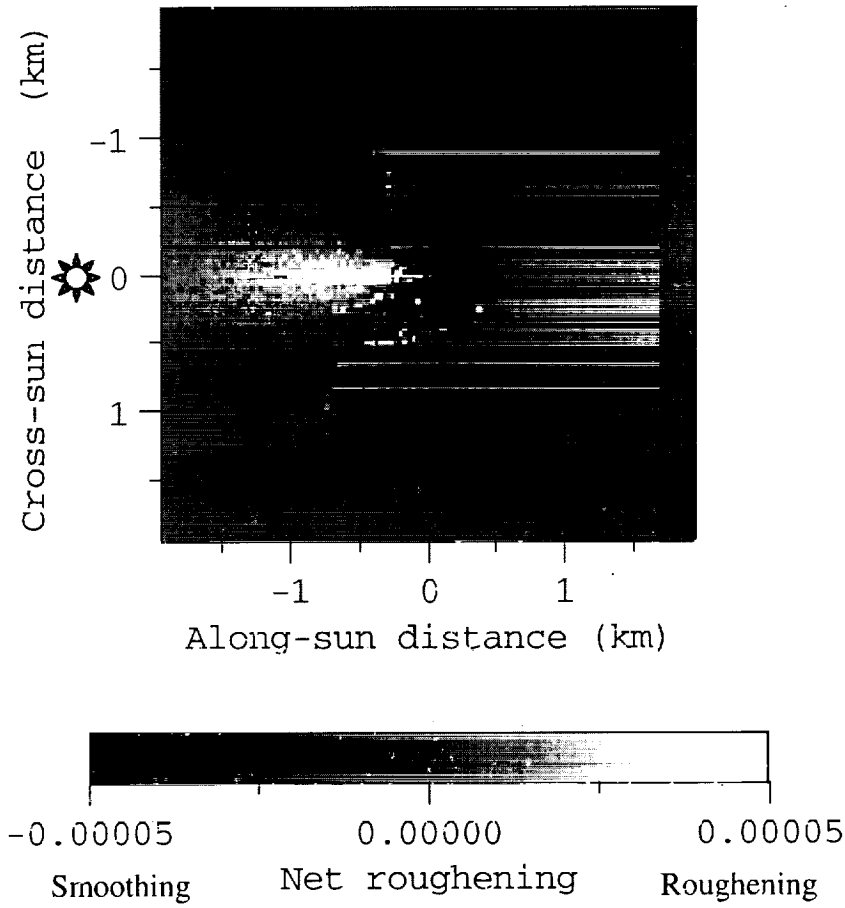
Cross-sun distance (km)
-1
0
1
-1
0
1
Along-sun distance (km)
-0.00005
0.00000
0.00005
Smoothing
Net roughening
Roughening

Figure 7.

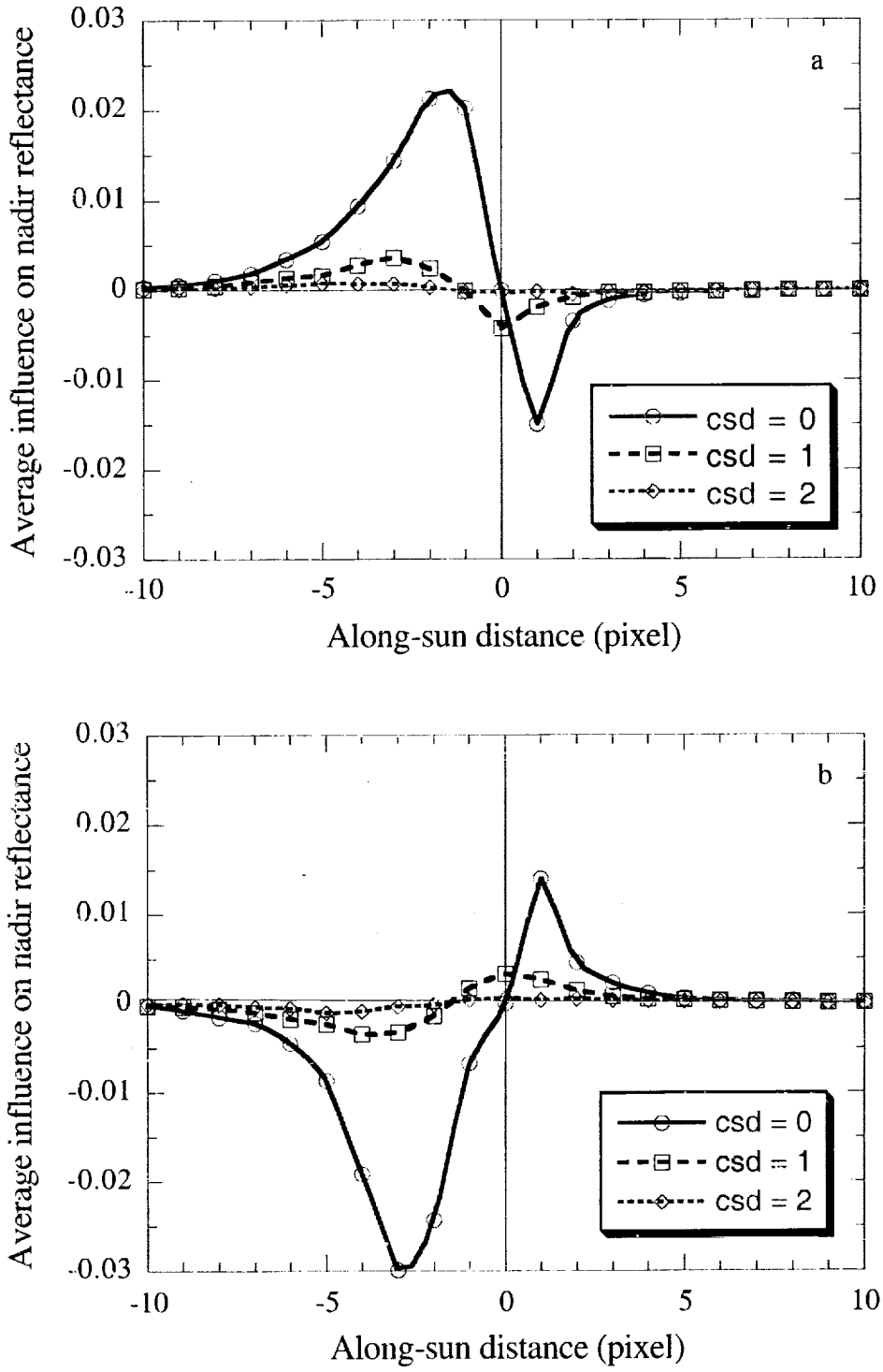
a
b
Average influence on nadir reflectance
Along-sun distance (pixel)
csd = 0
csd = 1
csd = 2
0.03
0.02
0.01
0
-0.01
-0.02
-0.03
-10
-5
0
5
10

Figure 8.

A Method to Analyze How Various Parts of Clouds Influence Each Other's Brightness

Tamás Várnai and Alexander Marshak
Joint Center for Earth Systems Technology

Prepared for the Journal of Geophysical Research-Atmospheres

Popular summary

This paper describes a method that can give us new information on the three-dimensional radiative interactions among various parts of clouds. Unlike current theoretical models, it can not only calculate the brightness of any given point, but can also determine which areas influence this brightness, to what degree, and through what mechanisms. After describing the proposed method, the paper illustrates its new capabilities both for detailed case studies and for the statistical processing of large datasets. Because the proposed method makes it possible, for the first time, to link areas to the radiative effects they have on other parts of clouds, future studies can use it to develop new radiative transfer parameterizations. These new parameterizations could perform fast calculations to consider horizontal radiative interactions in practical applications that are currently limited to vertical radiative processes-applications such as estimating cloud properties from satellite measurements and dynamical modeling of cloud development.